Chiral Plasma Instability in the Early Universe

Tina Kahniashvili
Carnegie Mellon University
Ilia State University

In collaboration with:
Axel Brandenburg, Emma Clarke, Andrew Long, Guotong Sun

PHENO2023
May 8, 2023

Physics Sacrosanct

Isotropy and homogeneity of the Universe:
Space-time in the Einstein Special and General Relativity theories has no preferred or distinguishable direction (frame);

Parity (Mirror) Symmetry
Invariance under reflection

Lorentz Symmetry
"The feature of nature that says experimental results are independent of the orientation or the boost velocity of the laboratory through space".

however

Puzzles to Solve

Why No Anti-Matter?

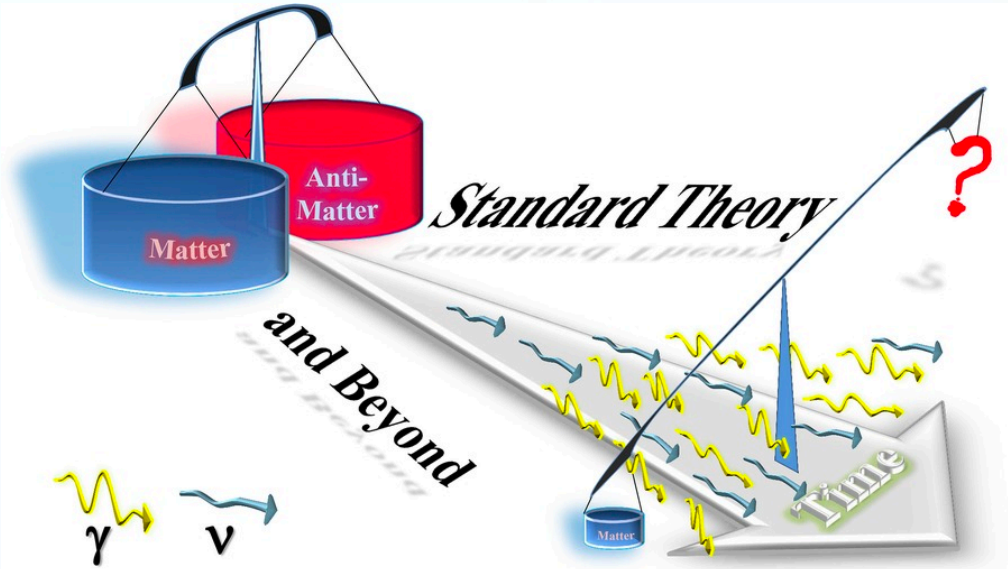

LHC Physics - 14 TeV

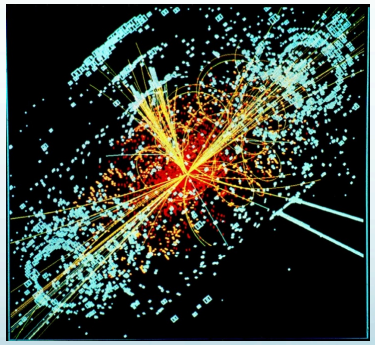

Physics Beyond Standard Model?

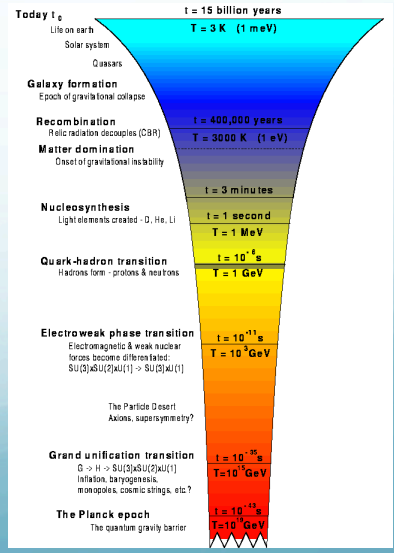

Do we have tools to test energies higher than LHC energy scales?

Cosmology up to $10^{16\text{-}19}$ GeV

New Physics: Cosmic Strings & Gravitational Waves

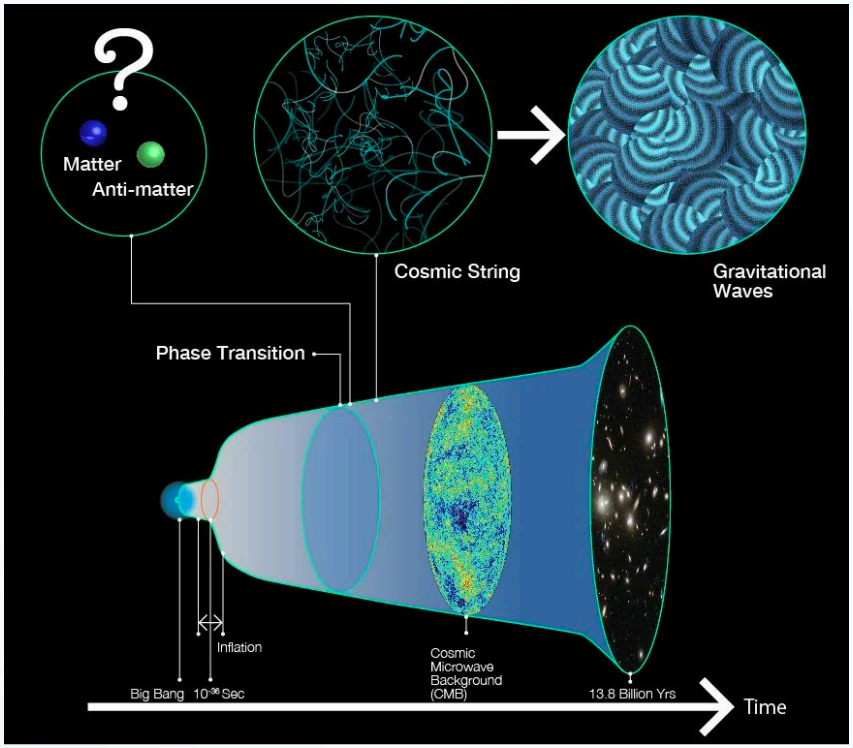

This graphic shows how cosmic strings formed after a phase transition in the early universe might have created gravitational waves detechttps://www.scientificamerican.com/article/cosmic-string-gravitational-waves-could-solve-antimatter-mystery/table by future observatories. Credit: R. Hurt/Caltech-JPL, NASA, and ESA Credit: Kavli IPMU - Kavli IPMU modified this figure based on the image credited by R.Hurt/Caltech-JPL, NASA, and ESA

https://www.scientificamerican.com/article/cosmic-string-gravitational-waves-could-solve-antimatter-mystery/

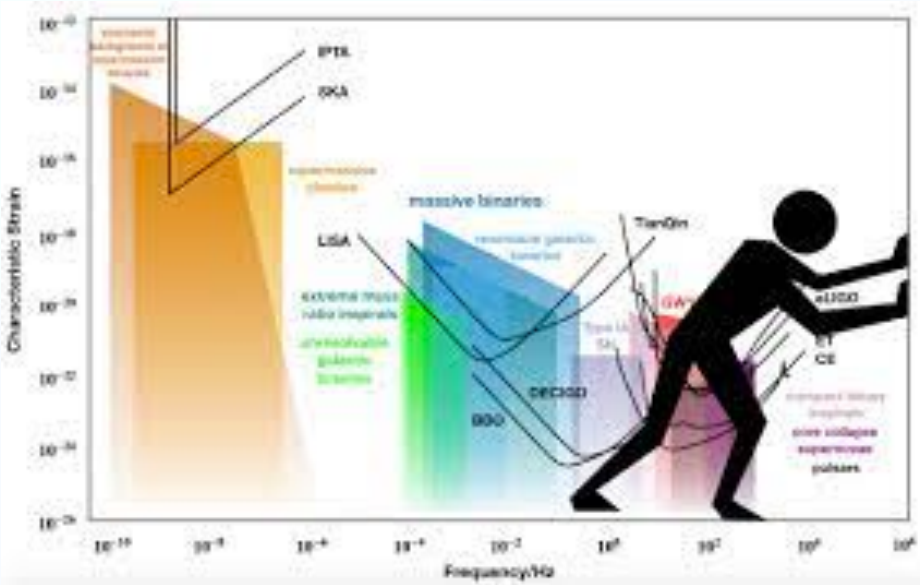

https://www.ctc.cam.ac.uk/activities/UHF-GW.php

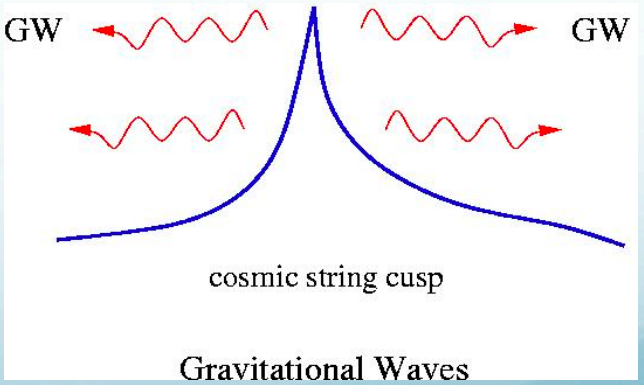

https://aether.lbl.gov/eunhwa_webpage_2/stringdynamics.html

Living Rev Relativ (2017) 20:2
https://doi.org/10.1007/s41114-017-0004-1

REVIEW ARTICLE

Detection methods for stochastic gravitational-wave backgrounds: a unified treatment

Joseph D. Romano[1] · **Neil. J. Cornish**[2]

A cosmological background produced by the superposition of a large number of independent gravitational-wave signals from the early Universe is expected to be Gaussian (via the central limit theorem), as well as isotropically-distributed on the sky. Contrast this with the superposition of gravitational waves produced by unresolved Galactic white-dwarf binaries radiating in the LISA band (10^{-4} Hz to 10^{-1} Hz). Although this confusion-limited astrophysical foreground is also expected to be Gaussian and stationary, it will have an anisotropic distribution, following the spatial distribution of the Milky Way. The anistropy will be encoded as amodulation in the LISA output, due to the changing antenna pattern of the LISA constellation in its yearly orbit around the Sun.

New Physics: Parity Violation in the Early Universe

- Motivation:
  - Matter-Antimatter Asymmetry – Baryogenesis and Leptogenesis
  - CP Symmetry Breaking
  - Chiral Magnetic Fields…

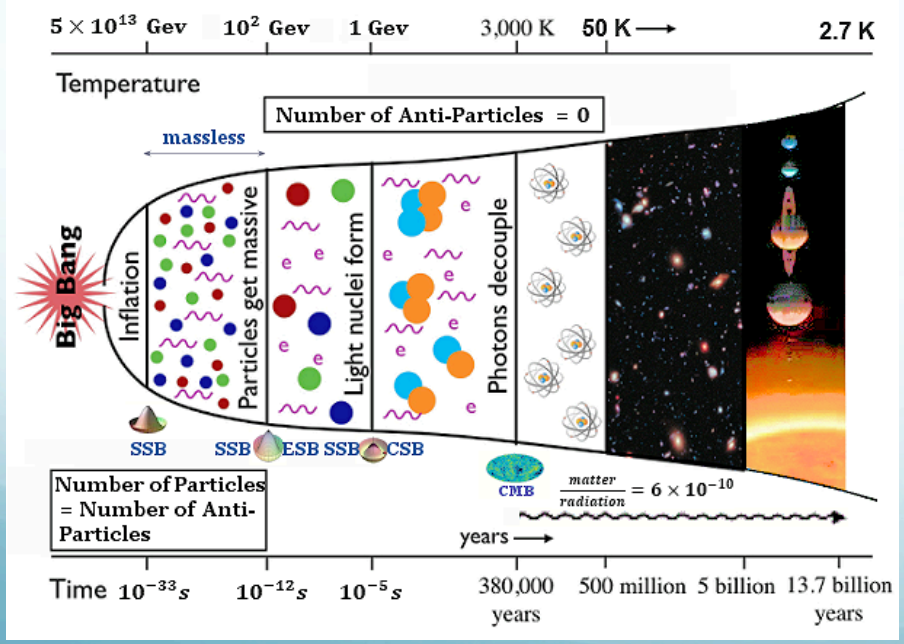

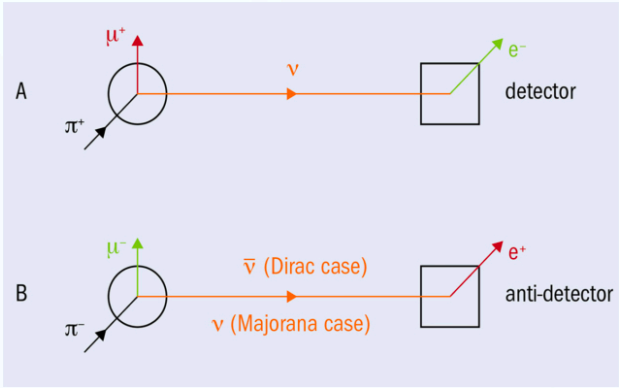

The pursuit of leptonic CP violation is based on comparing the rates for two CP-mirror-image processes. Credit: CERN

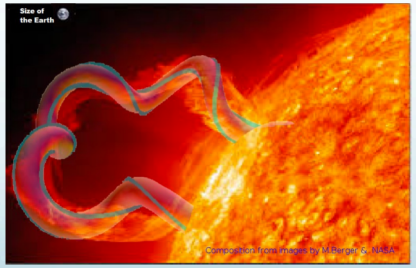

$$H_B(t) = \int d^3x \mathbf{A} \cdot \nabla \times \mathbf{A},$$

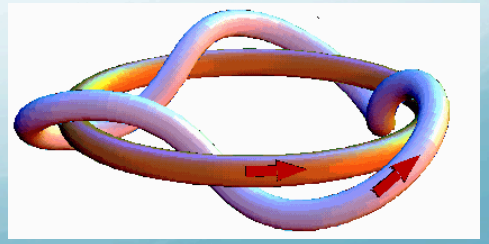

Blazars Spectra Observations:

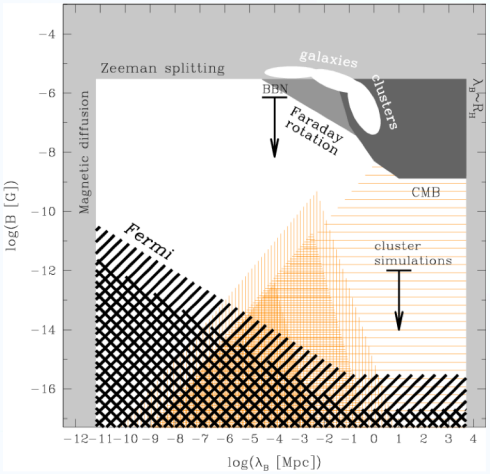

A. Neronov & E. Vovk," *Evidence for Strong Extra-galactic Magnetic Fields from Fermi Observations of TeV Blazars*", Science 328, 5974 (2010)

K. Dolag et al, *"Lower Limit on Strength and Filling Factor of Extragalactic Magnetic Fields"*, ApJ L. 727, L4 (2011)

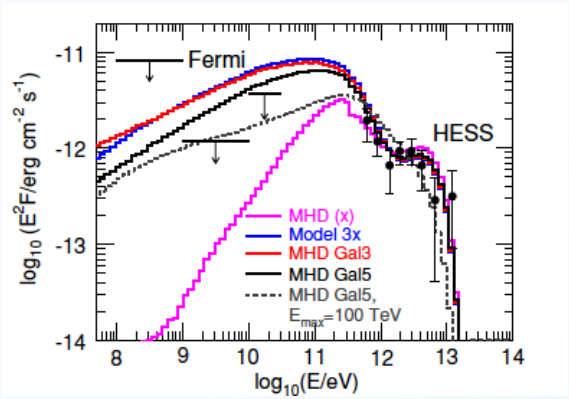

$$B \geq 10^{-15}\text{Gauss at } \lambda \geq 1\text{Mpc}$$

V. A. Acciari et al. [MAGIC Collaboration] "*A Lower Bound on Intergalactic Magnetic Fields from Time Variability of 1ES 0229+200 from MAGIC and Fermi/LAT Observations*", A&A, 670, 145 (2023)

S. Archambault et al. [VERITAS Collaboration], *"Search for Magnetically Broadened Cascade Emission From Blazars with VERITAS,"* Astrophys. J. 835 , 288 (2017).

M. Ackermann, et al. [Fermi-LAT Collaboration], *"The Search for Spatial Extension in High-latitude Sources Detected by the Fermi Large Area Telescope,"* Astrophys. J. Suppl. 237 , 32 (2018).

Gravitational Waves Polarization

- If the parity in the early universe is violated – relic gravitational waves are polarized.
- The standard model predicts un-polarized gravitational waves

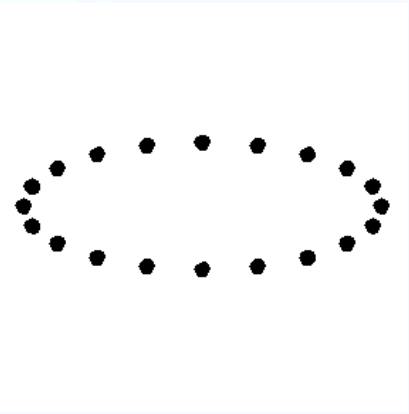

Linearly polarized + and X

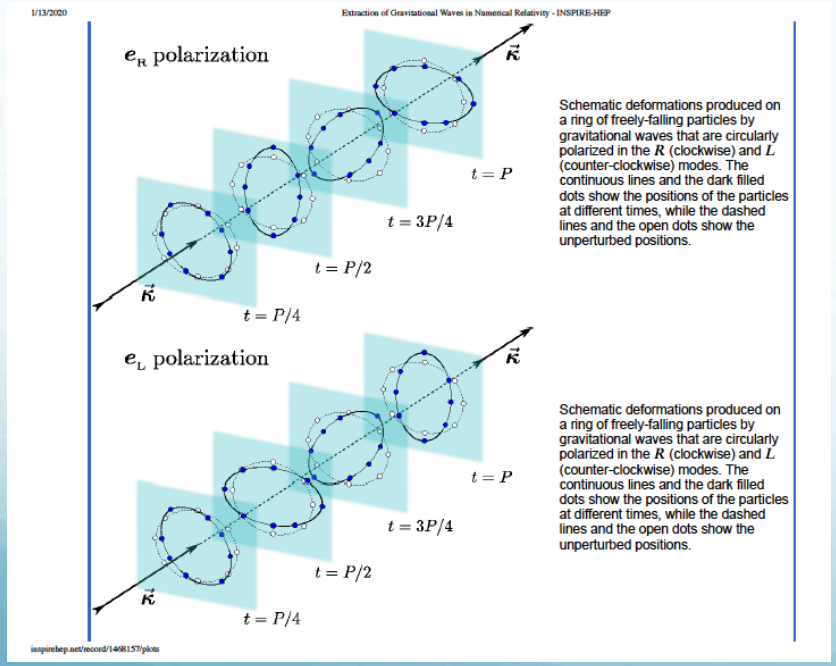

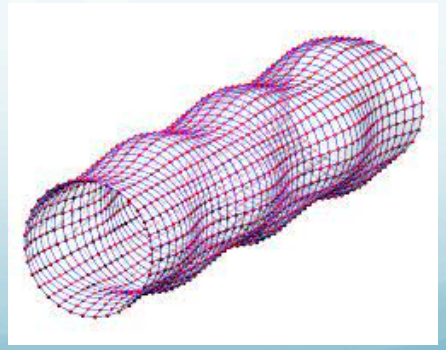

https://www.youtube.com/watch?v=F4stTzxYrN0

Detection Prospects

Measuring the net circular polarization of the stochastic gravitational wave background with interferometers

Valerie Domcke [a], Juan García-Bellido [b], Marco Peloso [c,d], Mauro Pieroni [b,e], Angelo Ricciardone [c], Lorenzo Sorbo [f], Gianmassimo Tasinato [g]

Abstract

Parity violating interactions in the early Universe can source a stochastic gravitational wave background (SGWB) with a net circular polarization. In this paper, we study possible ways to search for circular polarization of the SGWB with interferometers. Planar detectors are unable to measure the net circular polarization of an isotropic SGWB. We discuss the possibility of using the dipolar anisotropy kinematically induced by the motion of the solar system with respect to the cosmic reference frame to measure the net circular polarization of the SGWB with planar detectors. We apply this approach to LISA, re-assessing previous analyses by means of a more detailed computation and using the most recent instrument specifications, and to the Einstein Telescope (ET), estimating for the first time its sensitivity to circular polarization. We find that both LISA and ET, despite operating at different frequencies, could detect net circular polarization with a signal-to-noise ratio of order one in a SGWB with amplitude $h^2\Omega_{\rm GW} \simeq 10^{-11}$. We also investigate the case of a network of ground based detectors. We present fully analytical, covariant formulas for the detector overlap functions in the presence of circular polarization. Our formulas do not rely on particular choices of reference frame, and can be applied to interferometers with arbitrary angles among their arms.

- ✓ Dipolar anisotropy introduced by our proper motion, *Seto 2006* (for LISA and ET)
- ✓ Curvature of the Earth for ground based detectors, Seto & Taruya 2007, 2008

Domske et al. 2019:

In the present work we reconsider previous results by taking into account the full response functions and noise curves in the entire frequency band (for planar detectors). Moreover, we provide fully analytical and covariant expressions for the (parity-sensitive) response functions of a ground-based detector network.

Chirality: Parity Symmetry Breaking

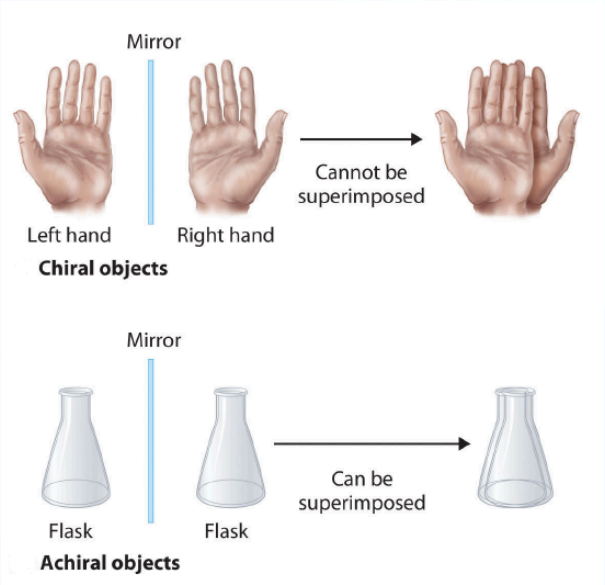

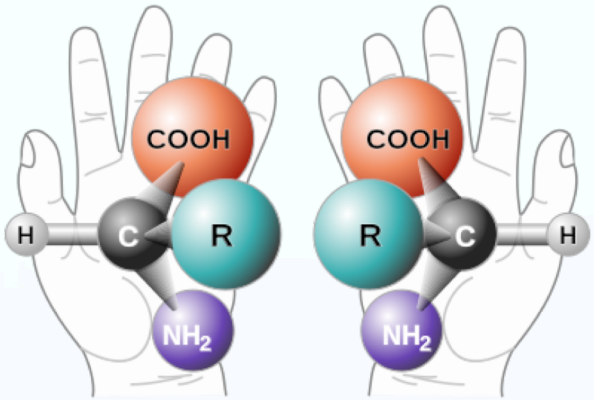

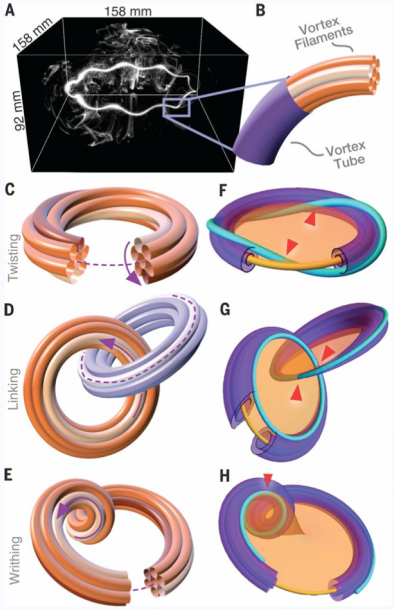

I call any geometrical figure, or group of points, 'chiral',

and say that it has chirality if its image in a plane mirror, ideally realized, cannot be brought to coincide with itself

Kinetic & Magnetic Helicity

https://www.science.org/doi/10.1126/science.aam6897

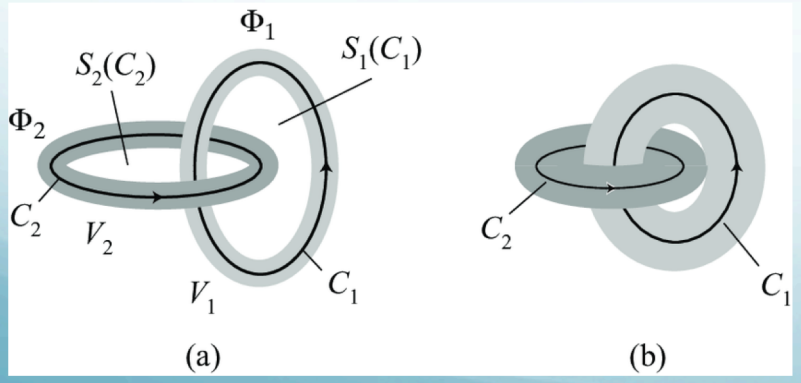

Kelvin

$$H^{\mathbf{M}} = \int_V \mathbf{A} \cdot \mathbf{B}\, dV.$$

in algebraic topology, the Hopf invariant is a homotopy invariant of certain maps between n-sphere

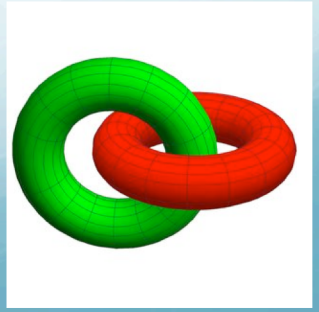

Hopf Invariant

Chiral Magnetic Effect

- ✓ Asymmetry between right- and left-handed fermions – amplification (exponential growth) of helical magnetic fields, chiral magnetic effect (CME), *Vilenkin 1980*

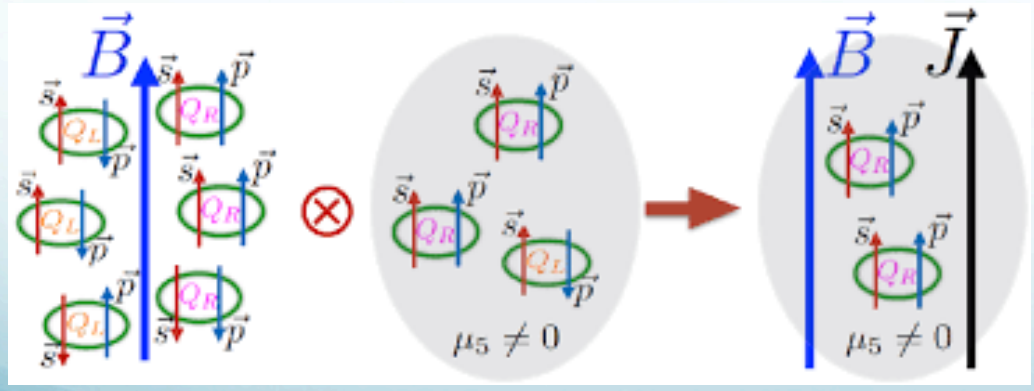

Kharzeev, Liao, Voloshin, Wang, 2015

- ✓ Magnetogenesis in the early universe – seed helical magnetic fields, *Boyarsky et al. 2012*
- ✓ Turbulent chiral magnetic inverse cascade in the early universe – *Brandenburg et al. 2017*

Chiral Turbulent Cascade

$$\frac{1}{2}\lambda\langle \boldsymbol{A}\cdot\boldsymbol{B}\rangle + \langle\mu\rangle = \text{const} \equiv \mu_0 \qquad \langle \boldsymbol{B}^2\rangle\,\xi_M \le \frac{\mu_0}{\lambda}$$

$$\mu_5 = 24\,\alpha_{em}\,(n_L - n_R)\left(\frac{\hbar c}{k_B T}\right)^2$$

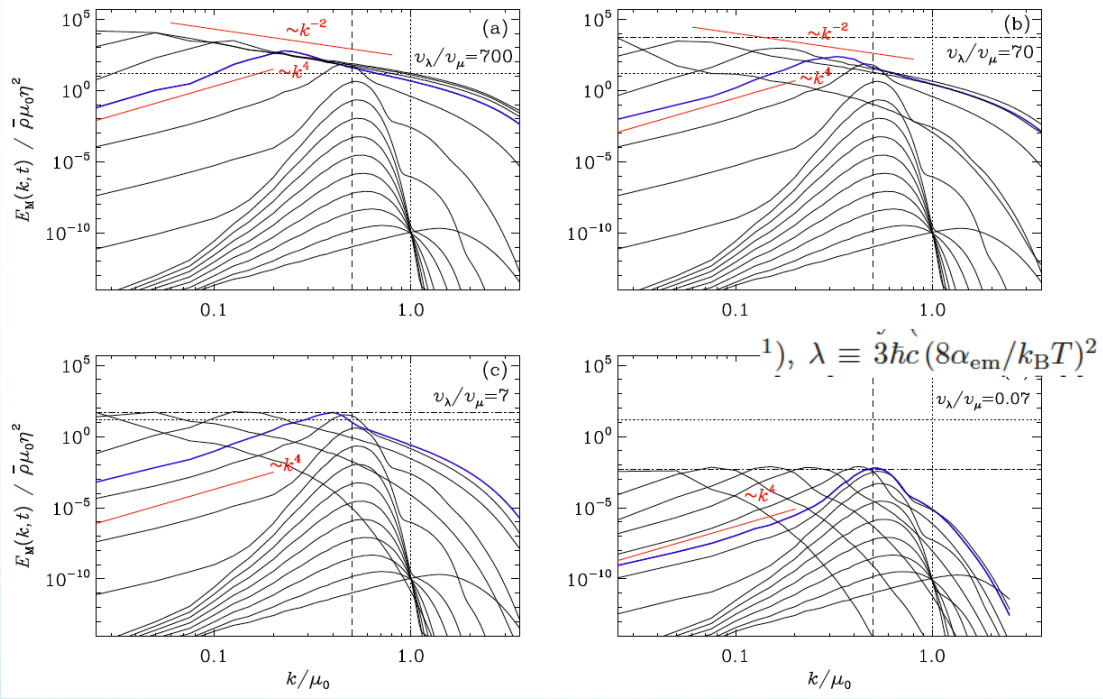

$^{-1}$), $\lambda \equiv 3\hbar c\,(8\alpha_{\rm em}/k_{\rm B}T)^2$

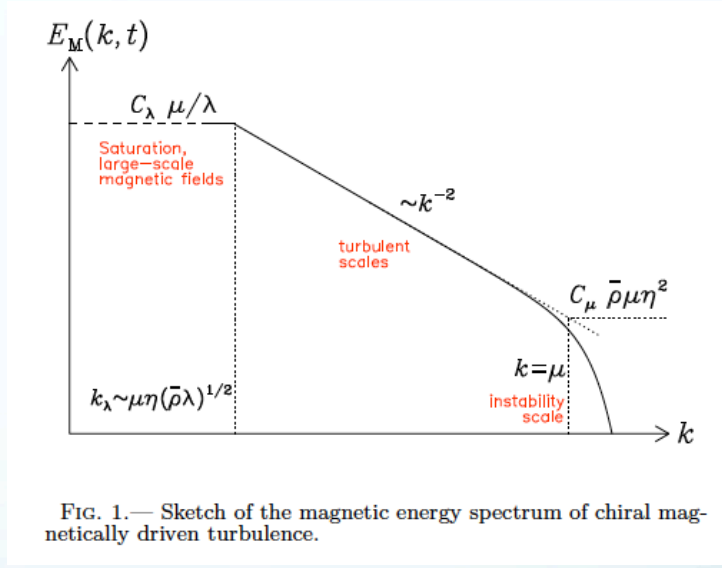

FIG. 1.— Sketch of the magnetic energy spectrum of chiral magnetically driven turbulence.

$$\eta k_1 < v_\mu < v_\lambda \quad \text{(regime I)},$$
$$\eta k_1 < v_\lambda < v_\mu \quad \text{(regime II)},$$

$$v_\lambda = \mu/(\lambda\bar{\rho})^{\frac{1}{2}} \qquad v_\mu = \mu\eta$$

$$\lambda = 3\hbar c(8\alpha_{EM}/k_B T)^2$$

$$\frac{\partial \boldsymbol{A}}{\partial t} = \eta\,(\mu\boldsymbol{B} - \boldsymbol{\nabla}\times\boldsymbol{B}) + \boldsymbol{U}\times\boldsymbol{B},$$

$$\frac{\mathrm{D}\mu}{\mathrm{D}t} = -\lambda\eta\,(\mu\boldsymbol{B} - \boldsymbol{\nabla}\times\boldsymbol{B})\cdot\boldsymbol{B} + D\nabla^2\mu - \Gamma_{\rm f}\mu,$$

$$\rho\frac{\mathrm{D}\boldsymbol{U}}{\mathrm{D}t} = (\boldsymbol{\nabla}\times\boldsymbol{B})\times\boldsymbol{B} - \boldsymbol{\nabla}p + \boldsymbol{\nabla}\cdot(2\rho\nu\mathbf{S}),$$

$$\frac{\mathrm{D}\rho}{\mathrm{D}t} = -\rho\boldsymbol{\nabla}\cdot\boldsymbol{U},$$

Brandenburg, et al. 2017

Chiral Gravitational Waves

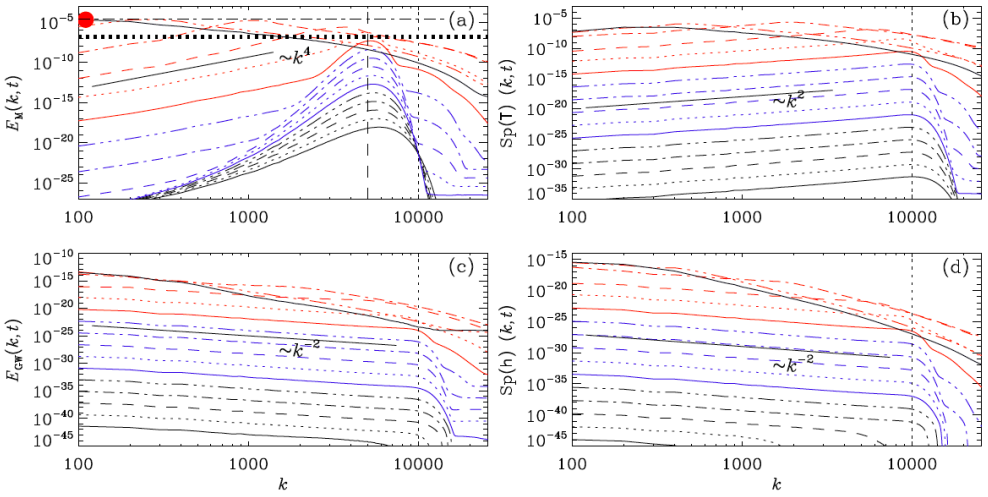

FIG. 6.— Time-evolving magnetic and GW energy spectra along with spectra of stress **T** and strain **h** for Run B1 (regime I) at $t-1=0.2$, 0.25, 0.3, 0.35, 0.4 in black, 0.45, 0.5, 0.55, 0.6, 0.65 in blue, 0.7, 0.75, 0.8, 0.9, 1.4 in red, and the time of maximum $\mathcal{E}_M$ at 1.9, again in black. In panel (a), the dotted horizontal line marks the level of $C_5\mu_{50}\eta^2$, and the horizontal dashed-dotted line the level of $C_\lambda\mu_{50}/\lambda$. Vertical dotted and dashed lines mark the positions of $2k_\mu=\mu_{50}$ and k_μ, respectively. The red filled symbol denotes the peak of $E_M(k)$ at the time of the magnetic maximum.

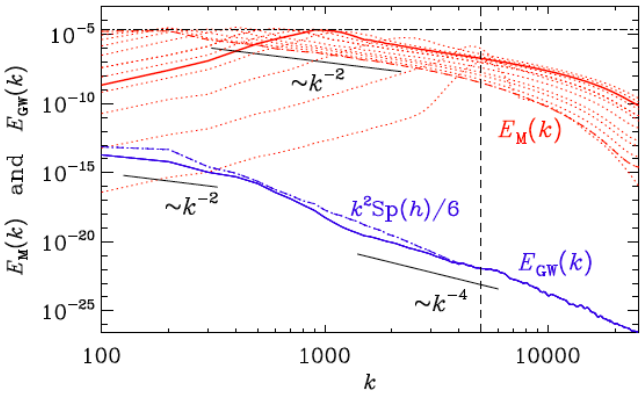

FIG. 2.— Magnetic and GW energy spectra for Run B1 with $\mu_{50}=10^4$, $\lambda=4\times10^8$, and $\eta=10^{-6}$, which is in regime I with $(v_\mu=0.01)<(v_\lambda=0.5)$. $E_M(k)$ (red) is shown at the time of magnetic maximum (solid, $t=1.92$), the time when the k^{-2} spectrum is most clear ($t=3$, dashed), and at selected other times (dotted, $t=1.71$, 1.77, 1.83, 1.89, 1.94, 2.00, 2.15, 2.32, 2.52, 2.74, and 3.00, while $E_{GW}(k)$ (solid blue) is from the simulation's end time ($t=14$), when it can be approximated by $k^2\mathrm{Sp}(\mathbf{h})/6$ (dashed-dotted blue). The black horizontal dashed-dotted line marks the saturation limit of Equation (10), μ_{50}/λ, and the vertical dashed line marks the position of k_μ.

$$\mathcal{E}_{GW}^{sat} \approx \left(q\mathcal{E}_M^{max}/k_{peak}\right)^2$$

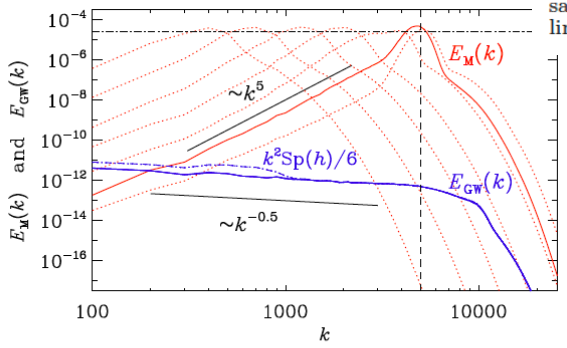

FIG. 3.— Similar to Figure 2, but for Run B10 with $\eta=10^{-3}$, which is in regime II with $(v_\mu=10)>(v_\lambda=0.5)$. $E_M(k)$ (solid red) is at the time when the magnetic energy has attained its maximum ($t=1.001$), dotted red lines show $E_M(k)$ at $t=1.0008$, 1.003, 1.008, 1.024, and 1.075, while $E_{GW}(k)$ is from the simulation's end time ($t=1.075$), when $E_{GW}(k)\approx k^2\mathrm{Sp}(\mathbf{h})/6$.

$$\mathcal{E}_{GW}^{sat} \propto v_\lambda^5 v_\mu$$

Brandenburg, et al. 2021

Chiral Plasma Instability in SM

- Accounting for spin-flip rate CPI may occur on temperatures higher than 100 TeV

$$\mathcal{H}_{\mathrm{M,CPI}} \simeq (4\times10^{-40}\mathrm{G^2Mpc}) \times \left(\frac{\alpha_Y}{0.01}\right)^{-1}\left(\frac{g_*}{106.75}\right)^{-1}\left(\frac{\mu_{Y,5}/T}{10^{-3}}\right)$$

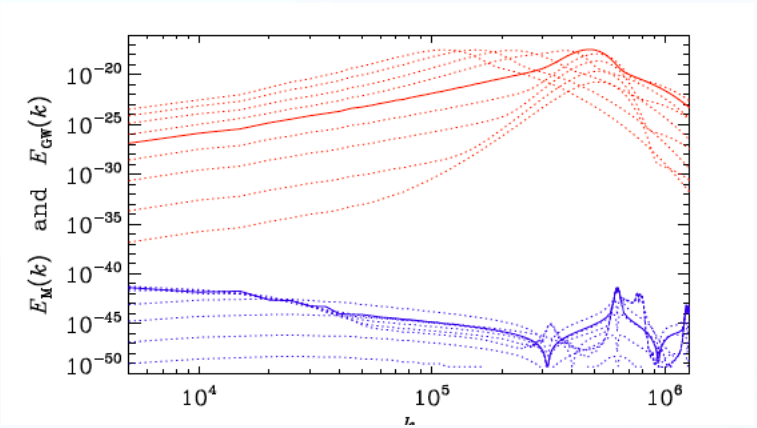

- Hypermagnetic field strength will be determined by $\mu_{Y,5}$
- The Hubble frequency

$$f_H = (1.6\times10^{-2}\,\mathrm{Hz})\left(\frac{T_*}{100\,\mathrm{TeV}}\right)\left(\frac{g_*}{106.75}\right)^{1/6}$$

- The total chiral asymmetry $\mu_{Y,5}$ value determines the wavenumber $k_{CPI} = 2\alpha_Y$ at which the CPI occurs.
- The gravitational wave spectrum typical frequency is determined by $\mu_{Y,5}$
- Gravitational waves will be circularly polarized

Brandenburg, Clarke, TK, Long, Sun
work in progress

Conclusions and Take Home Comments

- The CPI generated magnetic fields agrees with the lower limits from FERMI/Veritas/MAGIC only marginally
- Gravitational waves astronomy opens new widows to test fundamental symmetries, especially parity violation: gravitational waves chirality will be a direct manifestation of parity symmetry breaking
- For the cosmological parameters allowed by the SM the CPI gravitational waves frequency is beyond range accessible by LIGO, and in addition it is too small to be detectable by current/future missions
- What extensions of SM will allow us solve cosmological puzzles?

Thank You

Work is partially supported by:
- NASA ATP #80NSSC22K0825
- SRNSFG #FR/19-8306